**Electronic Supplementary Information**

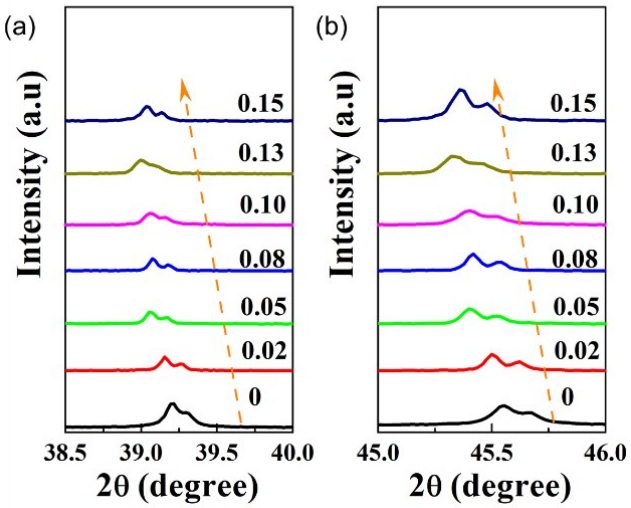


Figure S1. Representative diffraction peaks of (a) $\{111\}_p$ and (b) $\{200\}_p$ for all composition in BF-BT-xBLN ceramics.

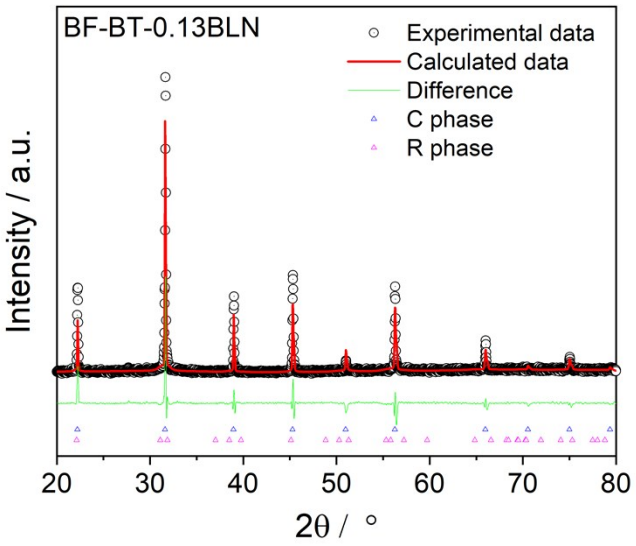


Figure S2 Full-pattern refinement data for BF-BT-0.13BLN ceramic using mixed-phase of *R3c* rhombohedral and *Pm3m* Cubic.

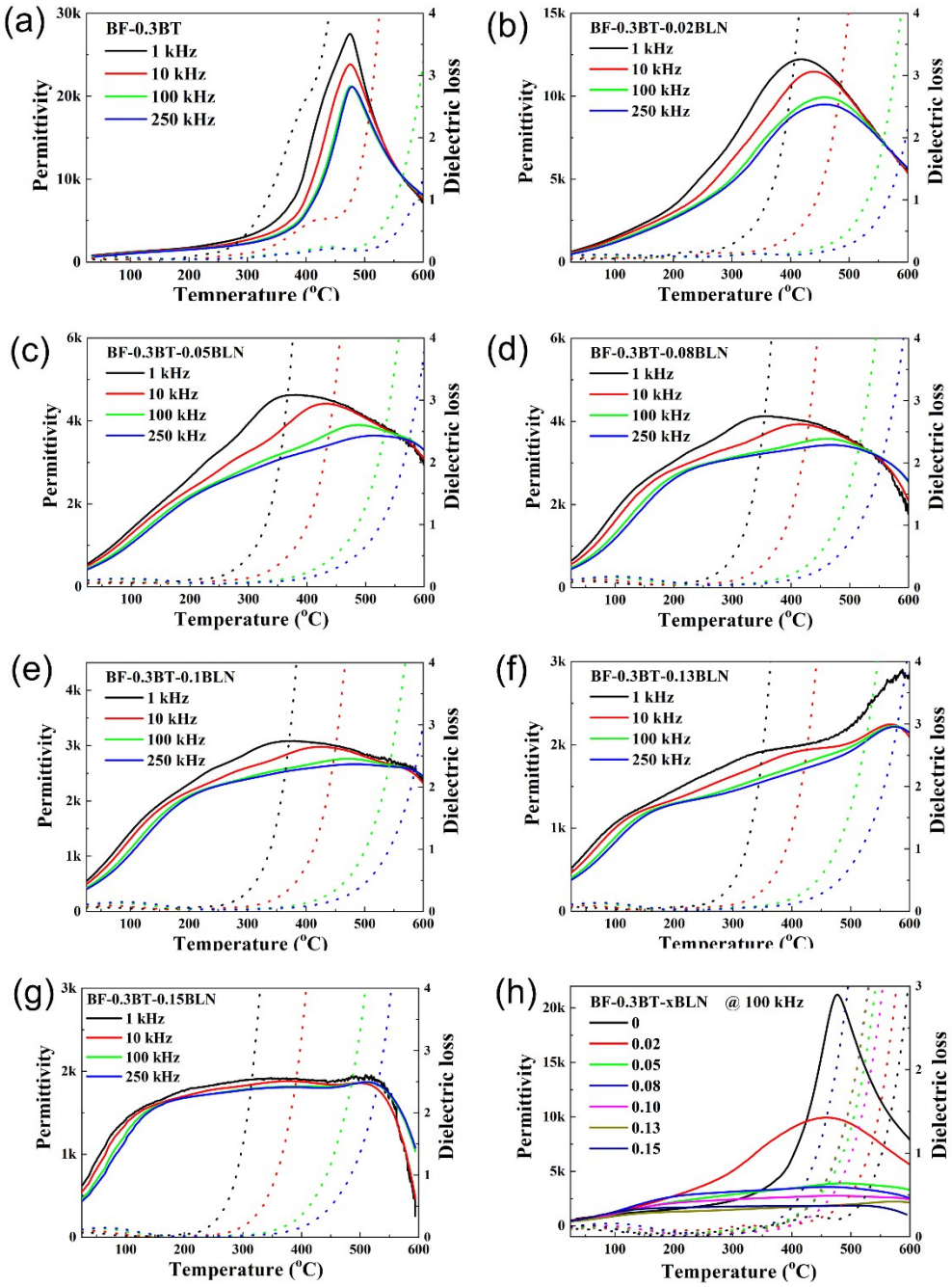


Figure S3. (a-g) Temperature-dependent permittivity and dielectric loss data at a frequency of 1, 10, 100 and 250 kHz for BF-0.3BT-xBLN ceramics. (h) Temperature-dependent permittivity and dielectric loss data for BF-BT-xBLN ceramics at 100 kHz.

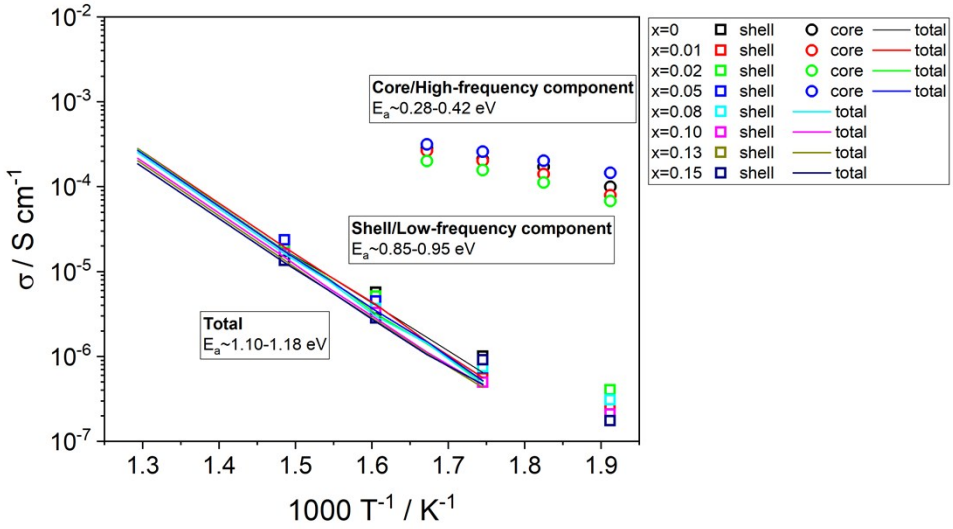


Figure S4. Arrhenius plots of core, shell and total conductivity values for BF-BT-xBLN ceramics.

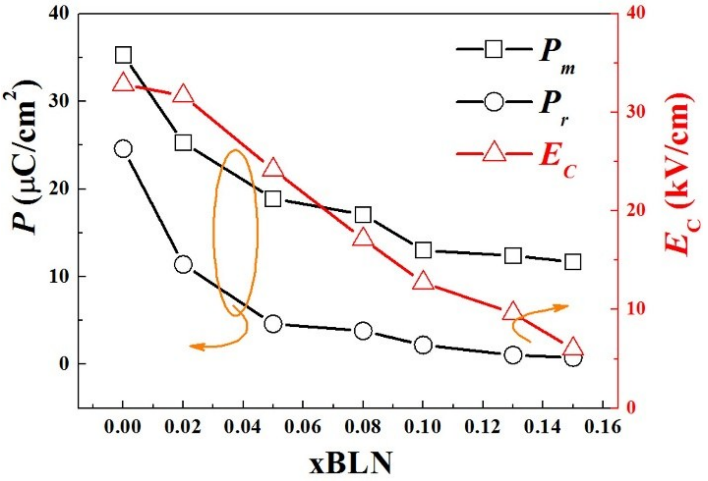


Figure S5. Changes of $P_m$, $P_r$ and $E_c$ for BF-BT-xBLN ceramics

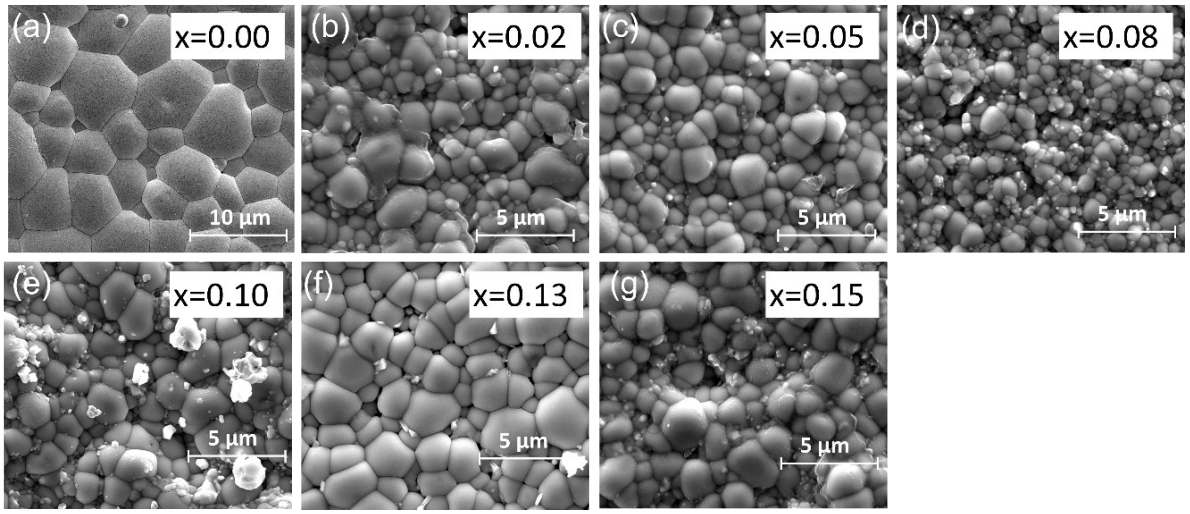


Figure S6 SEM surface micrographs for BF-BT-xBLN (x=0.00-0.15) ceramics.

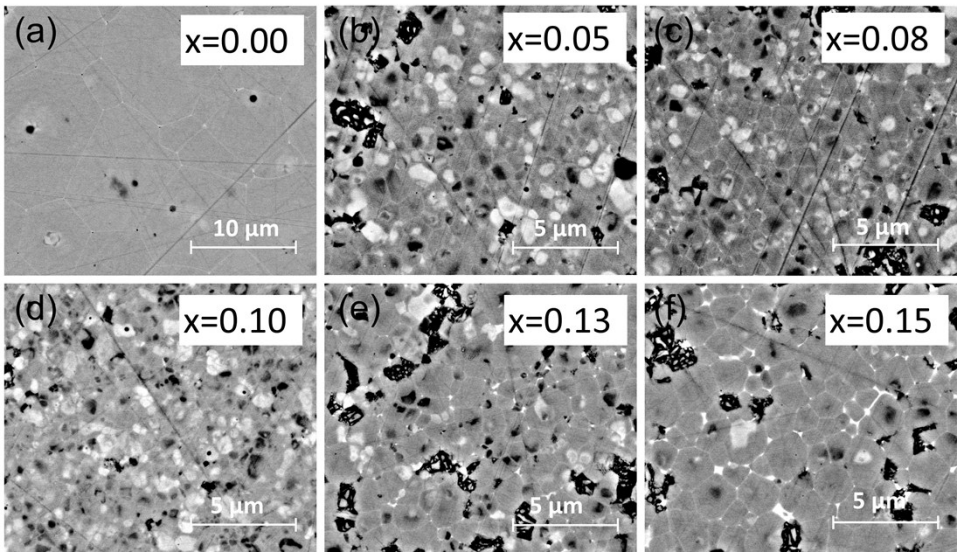


Figure S7 BSE micrographs of polished surfaces for BF-BT-xBLN (x=0.00-0.15) ceramics.

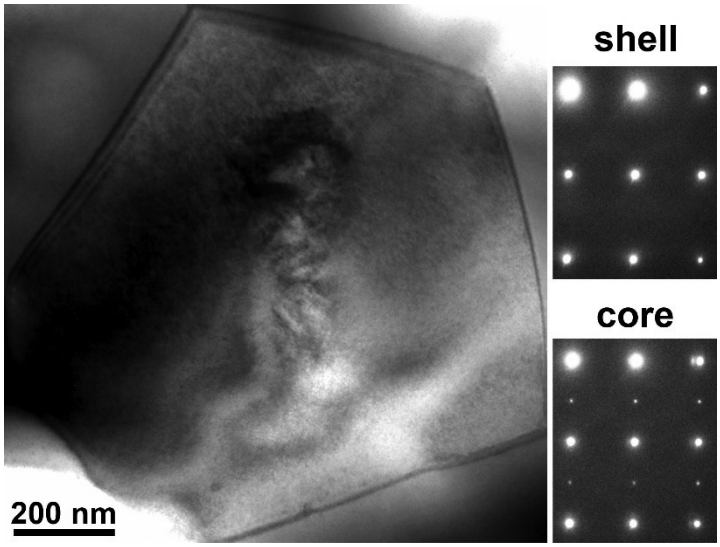


Figure S8. TEM domain morphology with diffraction spots for BF-BT-0.13BLN ceramics.

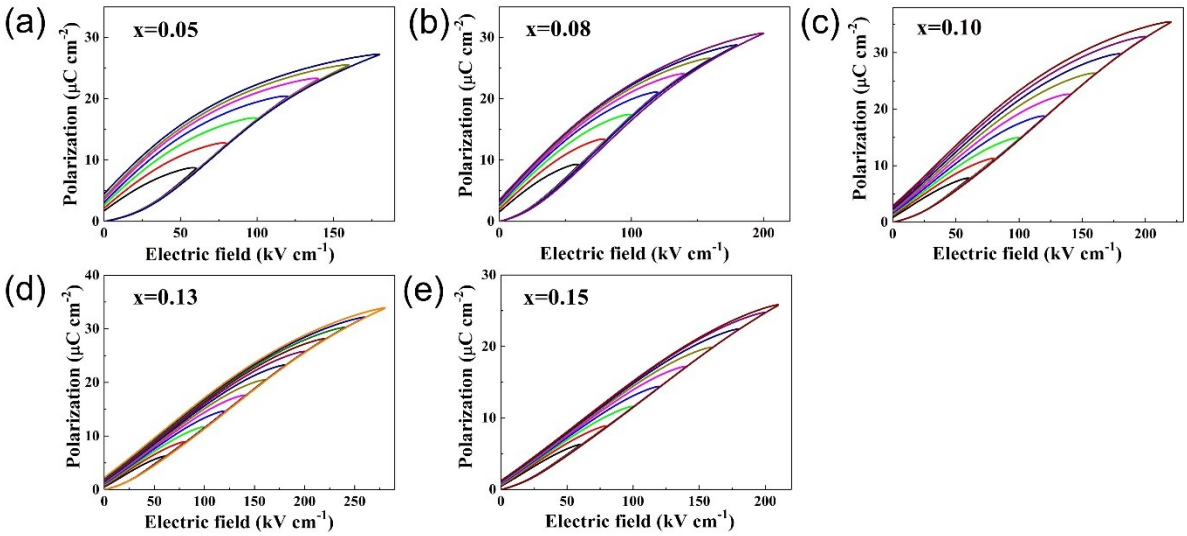


Figure S9. Unipolar P-E loops up to $E_{max}$ for BF-BT-xBLN ceramics.

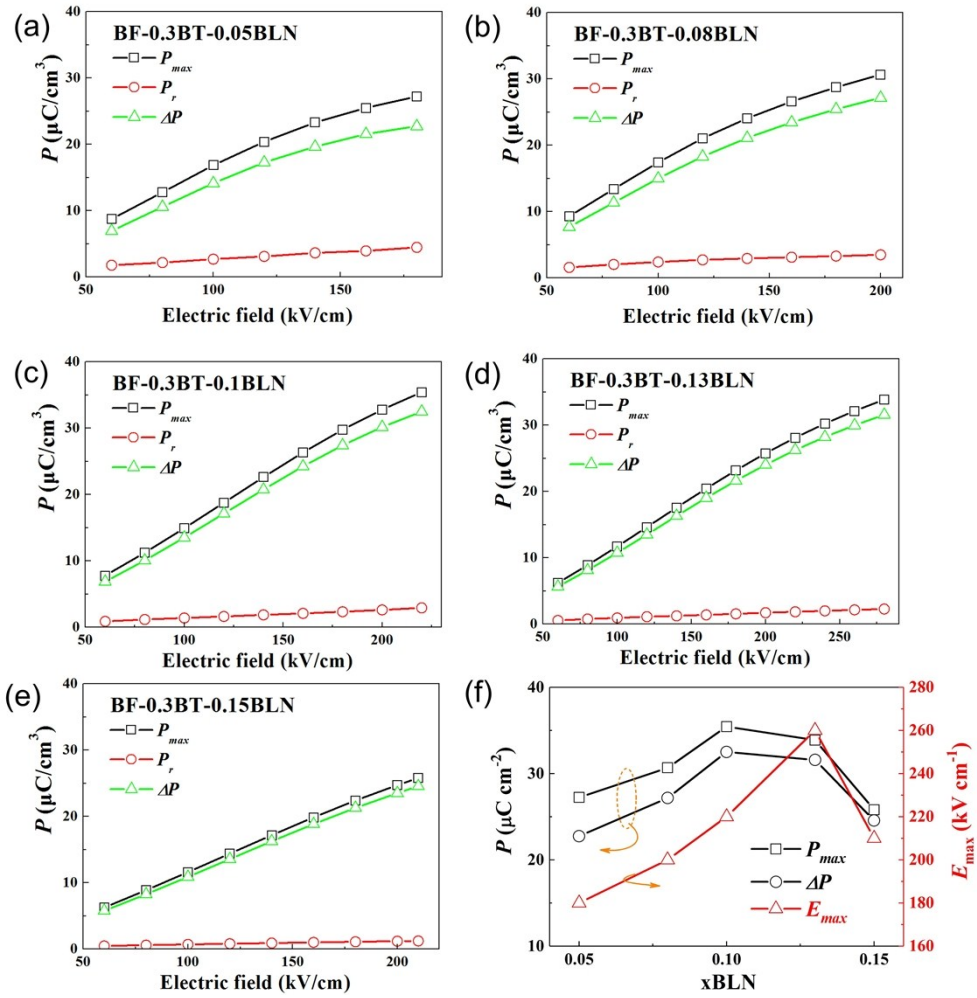


Figure S10. (a-e) $P_{max}$, $P_r$ and $\Delta P$ versus electric field for BF-0.3BT-xBLN ceramics. (f) Changes of $P_{max}$, $\Delta P$ and $E_{max}$ as function of BLN concentration.

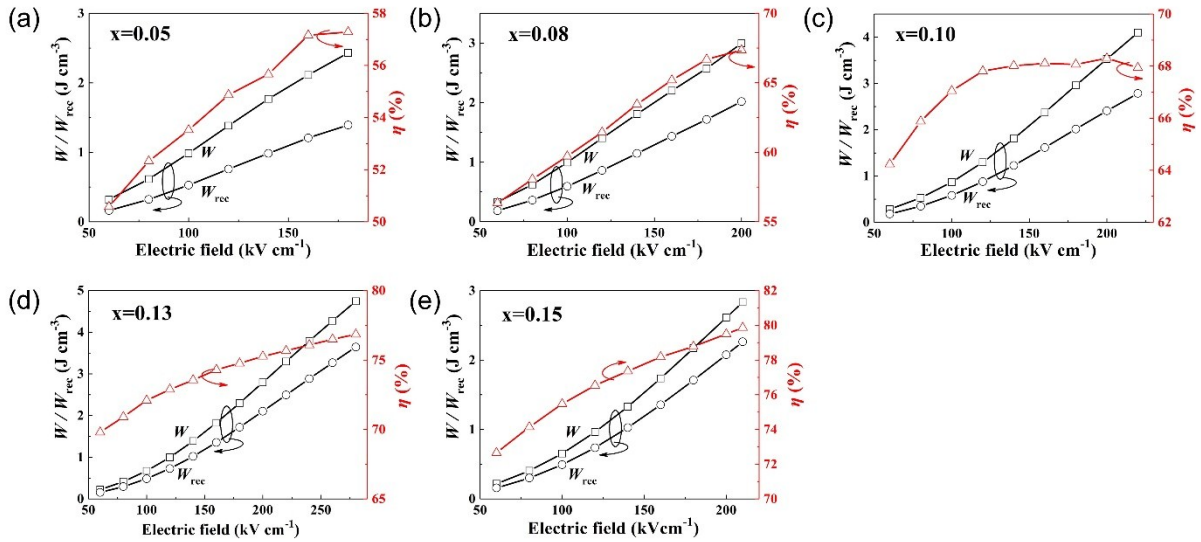


Figure S11. (a-e) W, $W_{rec}$ and η at different electric fields for BF-BT-xBLN ceramics.

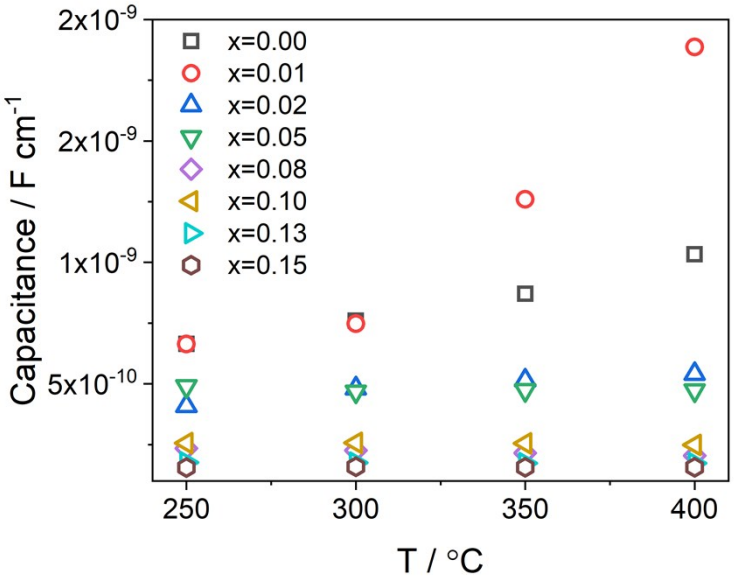


Figure S12. Variation in capacitance associated with the dominant M'' peak in the M'' spectra for BF-BT-xBLN ceramics in the temperature range ~ 250 to 400 °C.

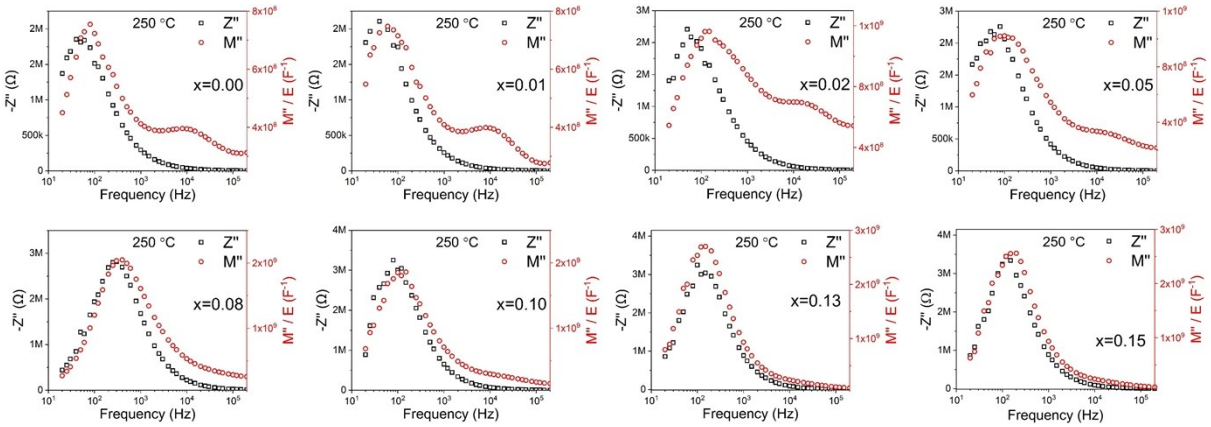


Figure S13. Combined Z'' and M'' spectroscopic plots at 250 °C for BF-BT-xBLN ceramics.

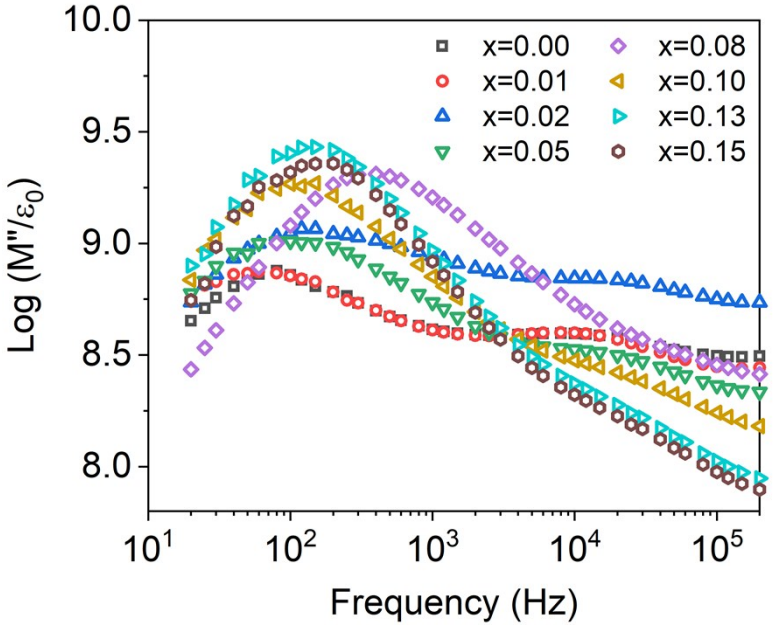


Figure S14. Log M'' verses log f plots at 250 °C for BF-BT-xBLN ceramics.

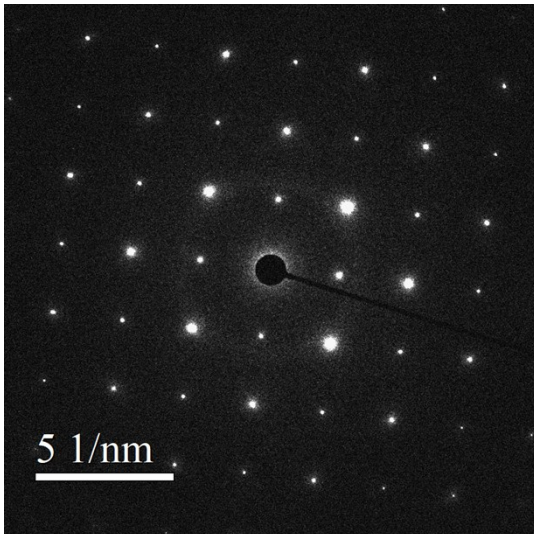


Figure S15. <100> SAD pattern obtained from the BF-BT-13BLN ceramic.

| Composition | Space group | Lattice parameter | | | Phase fraction / % | $R_{wp}$ | GOF |
|---|---|---|---|---|---|---|---|
| | | a / Å | b / Å | c / Å | | | |
| BF-BT-0.13BLN | *R3c* | 5.6316(7) | 5.6316(7) | 13.9806(2) | 13.6 | 7.85 | 1.86 |
| | *Pm3m* | 4.0305(10) | 4.0305(12) | 4.0305(7) | 86.4 | | |

Table S1. Refined structural parameters for BF-BT-0.13BLN ceramics. *GOF: goodness of fitting

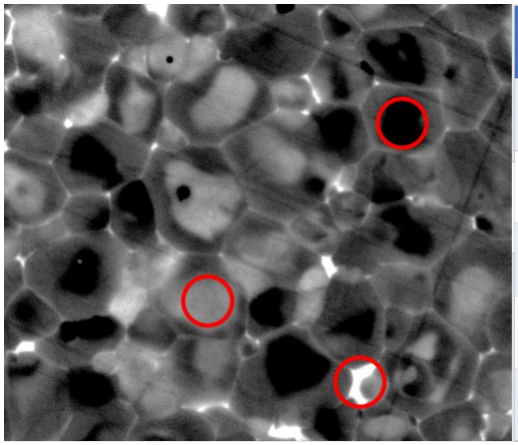

| | GB bright | White | Dark | Overall |
|---|---|---|---|---|
| **Bi** | 33.8% | 20.5% | 13.2% | 16.1% |
| **Fe** | 3.5% | 15.8% | 8.9% | 12.5% |
| **Ba** | 1.9% | 4.4% | 8.7% | 6.9% |
| **Ti** | 2.2% | 5.1% | 9.1% | 6.5% |
| **Results** | Bi-rich | Bi/Fe-rich | Ba/Ti-rich | N/A |

Table S2. Atomic percentage (excl. O) of BF-BT-0.13BLN quantified from EDS spectra from the ringed regions.

| **Materials** | **$W_{rec}$ / J cm$^{-3}$** | **η / %** | **ref** |
|---|---|---|---|
| BT-BLT | 2.2 | 89 | 19 |
| NBT-SBT | 9.5 | 92 | 31 |
| Nd-BF-BT | 6.74 | 77 | 40 |
| BF-BT-NZZ | 10.5 | 87 | 45 |
| BT-BZNT | 8.13 | 95 | 23 |
| BT-BZNT | 10.12 | 89 | 22 |
| Ba, Zr-PLZT | 6.8 | 61.2 | 70 |
| BT-BLN | 4.5 | 92 | 21 |
| BT-BS | 6.1 | N/A | 71 |

Table S3. $W_{rec}$ vs. η for different lead-free multilayers